The Effect of Electric Cross-Talk in Retinal Neurostimulation

Paul B. Matteucci,[1] Alejandro Barriga-Rivera,[1] Calvin D. Eiber,[1] Nigel H. Lovell,[1] John W. Morley,[2,3] and Gregg J. Suaning[1]

[1]Graduate School of Biomedical Engineering, University of New South Wales, Sydney, Australia
[2]School of Medicine, Western Sydney University, Sydney, Australia
[3]School of Medical Science, University of New South Wales, Sydney, Australia

Correspondence: Gregg J. Suaning, Graduate School of Biomedical Engineering, Level 5, Samuels Building, University of New South Wales, NSW 2052, Australia; g.suaning@unsw.edu.au.

PBM and AB-R contributed equally to the work presented here and should therefore be regarded as equivalent authors.

Submitted: October 14, 2015
Accepted: December 4, 2015

Citation: Matteucci PB, Barriga-Rivera A, Eiber CD, Lovell NH, Morley JW, Suaning GJ. The effect of electric cross-talk in retinal neurostimulation. *Invest Ophthalmol Vis Sci*. 2016;57:1031–1037. DOI:10.1167/iovs.15-18400

Purpose. To investigate the efficacy of electric field shaping in modulating the extent and activation threshold in retinal neurostimulation. This study aims to quantify the interference of neighboring stimulation sites by assessing the shift in the activation threshold produced by a concomitant interfering stimulus.

Methods. Electrical stimuli were applied to healthy retinae in a feline model ($n = 4$) using a 24-channel electrode array surgically implanted in the suprachoroidal space. A 96-channel penetrating electrode array was used for recording cortical responses to a number of stimulation paradigms. Data were analyzed offline. Concurrent monopolar and hexapolar stimuli were delivered at primary and interfering sites separated by up to 2.19 mm to evaluate electric cross-talk. The spike rate was fit to a sigmoidal curve to estimate the P_{50} threshold. The slope of the linear regression of the P_{50} value versus interfering current level was considered as a measure of cross-talk.

Results. Concurrent monopolar stimulation produced a proportional drop in the P_{50} of approximately 20% of the interfering current level in presence of a primary monopolar and hexapolar stimulus. On the other hand, hexapolar interference did not alter activation thresholds at the primary site.

Conclusions. Hexapolar stimulation reduces electric cross-talk between neighboring sites and represents a technique to reduce interference between individual stimulation sites. In contrast, concurrent monopolar stimulation produces a reduction of the activation threshold of stimuli delivered nearby. Thus, a single source of subthreshold monopolar charge injection can provide benefit in the form of significant threshold reduction simultaneously at multiple stimulation sites.

Keywords: retinal neurostimulation, retinal crosstalk, electrophysiology, field overlapping, neuromodulation, visual prosthesis

Investigations into the delivery of visual percepts to the blind through electrical neuromodulation have led to increasing promise that a technology-based therapy may soon be effective in restoration of functional vision.[1–3] As visual neuroprostheses continue to improve, the key requirements of these devices are becoming increasingly clear.[4–6] Among others, increased visual acuity and frame rate have important roles in providing meaningful percepts to describe the visual scene.[7] These requirements boost efforts to develop efficacious stimulation strategies, including current steering techniques.[8–10]

In a previous study, Dumm et al.[8] investigated simultaneous stimulation at different sites to elicit perception associated with so-called "virtual electrodes," opening the door to increased visual acuity. Intermediate additional phosphene perceptions may be elicited between those created by physical electrodes, which may benefit visual prosthesis recipients. Because those electrodes being used to create an intermediate perception will not be available to stimulate at their site, an increased frame rate will be required to compensate for this limitation. Note that simultaneous multiple-electrode stimulation can be engineered as a single stimulus, which combined with time-multiplexing stimulation may relax requirements on frame rate.[10]

Other studies have shown, in silico, in vitro, and in vivo, that a combined hexapolar (the active electrode is surrounded by six electrodes arranged hexagonally, which recover the stimulating current) and monopolar return configuration, known as quasi-monopolar (QMP), provides focused stimulation with reduced current threshold.[9,11–13] The QMP configuration, through the reduced activation threshold it achieves, decreases the likelihood of creating adverse electrochemical reactions, which may assist designing more densely arranged electrode arrays.

Current steering has shown excellent results in auditory prosthesis adding extra pitch percepts[14]; thus, increasing spectral resolution.[15] In particular, a variant of the QMP approach was explored in cochlear implants through partial tripolar excitation showing increased loudness perception,[16] leading to the idea that such electric field forming approaches have use in myriad areas of neuroprosthesis. In a context of continuous development and improvement of stimulation devices with cutting-edge capabilities, particularly in the

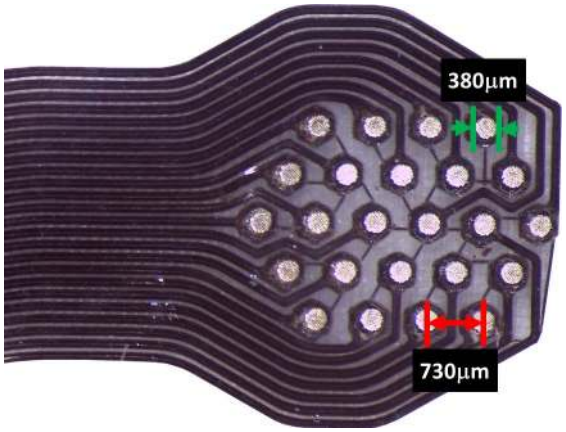

FIGURE 1. Stimulating electrode array consisting of 24 platinum electrodes with a diameter of 380 μm arranged hexagonally with electrode spacing (*center* to *center*) of 730 μm.

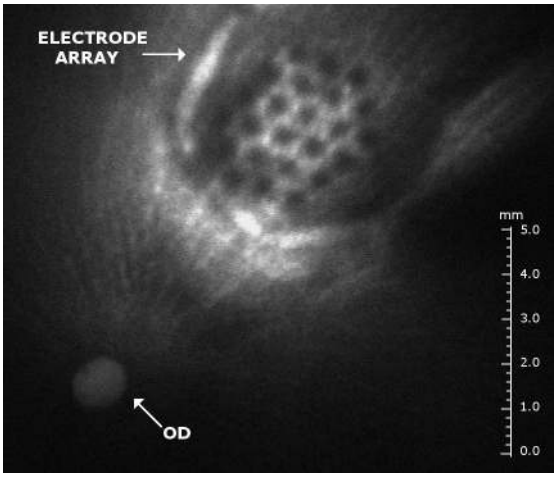

FIGURE 2. Example of infrared fundus imaging performed after surgical implantation of the 24-channel electrode array. The tip of the electrode array was located approximately 5 mm from the center of the optic disc.

quantity of stimulating electrodes, series stimulation approaches are rapidly becoming obsolete. For this reason, there is a clear need for faster and more efficient means of stimulus delivery. In particular, an exacerbating issue in prior attempts at parallel stimulation has been the interference that one site of stimulation has on others. In the literature, this also is referred to as cross-talk.[11,17] Approaches to reduce interference from concomitant stimulation have considered spatial isolation of stimuli by confining the electric field using current focusing techniques,[9,18,19] time-multiplexing strategies,[1,20,21] or both.

The focus of this study is the assessment of the effect of interference at one site of stimulation as a result of the concomitant delivery of stimuli elsewhere. Owing to its well documented visual system, a cat model was chosen.[18] To quantify the extent of interference, namely cross-talk, stimulation threshold shift was measured using linear regression when a repertoire of concurrent stimulation paradigms was applied at a different site than the site targeted for activation. In so doing, the efficacy of various stimulation strategies in minimizing cross-talk was evaluated.

Materials and Methods

Stimulating Electrode Array

A custom stimulating electrode array was fabricated in the authors' laboratory following the procedure reported previously in the scientific literature.[22,23] Briefly, a picosecond pulse, Nd:YAG laser micro-machining process was applied to form the electrode and interconnecting wires from 25-μm thick platinum foil. The platinum foil was previously laminated to a polydimethylsiloxane (PDMS) substrate reinforced with polyethylenetherephalate (PET) mesh to improve its mechanical strength. Following the application of a covering layer of PDMS, electrode surfaces were exposed using a 193-nm wavelength excimer laser resulting in an array of 24 electrodes arranged in a hexagonal mosaic. Each circular electrode had an exposed diameter of 380 μm and a center-to-center distance of 730 μm, as shown in Figure 1. Aside from the hexagon being an efficient geometry in which to pack circular structures onto a planar surface, previous studies have shown that the hexagonal unit comprising a central stimulating electrode with six surrounding return electrodes provides an effective means of isolation of stimuli.[13]

Animal Preparation and Surgery

Four normally-sighted adult cats (*Felis catus*) of postnatal age between 557 and 908 days (median 594 days) and having a weight of 4.1 to 6.1 kg (median 5.2 kg) were included in this study. All procedures described herein were performed with the approval of the UNSW Animal Care & Ethics Committee and in compliance with the Australian code for care and use of animals for scientific purposes and the ARVO Statement for the Use of Animals in Ophthalmic and Vision Research.

Surgical preparation has been described previously.[9] Briefly, anesthesia was induced via intramuscular injection of ketamine (20.0 mg/kg) and xylazine (1.0 mg/kg) and maintained via constant intravenous infusion of alphaxalone (2.0–4.0 mg/kg/h) in 10 mL solution with 20 mL of 5% glucose and 20 mL of Hartmann's solution and inhaled isoflurane (0%–3% in equal parts of oxygen and air). Intraarterial and intravenous catheters were used for monitoring blood pressure and administration of fluid and pharmacological agents, respectively. Dexamethasone (intramuscular, 1.5 mg/kg), enrofloxacin (intramuscular, 0.1 mL/kg), and atropine (subcutaneous, 0.2 mg/kg) were administered daily. To ensure adequate respiration, a tracheostomy was performed, the animal was placed on mechanical ventilation, and expired CO_2 levels were monitored. Core temperature was measured via a thermal probe and regulated by way of an air-filled heated pillow beneath the animal.

The stimulating electrode array was advanced into the suprachoroidal space via a scleral incision 7 mm posterior to the limbus. Depth markers on the array aided in the positioning of the array's tip at the area centralis and its location was verified after surgery by infrared fundus imagery using an in-house-built system, as shown in Figure 2. Pupillary dilation was achieved by hydroxypropyl methylcellulose (HPMC) in saline solution beneath zero power contact lenses.

Following placement of the cat within a stereotaxic frame, a craniotomy and durotomy were performed contralateral to the implanted eye using coordinates from Tusa et al.[24]

Experimental Setup and Mapping

The primary and secondary visual cortices (areas 17 and 18) were mapped with a 2.3-mm in diameter epicortical platinum ball electrode. This electrode was interfaced to a RZ2 TDT multichannel recording system (Tucker Davis Technologies,

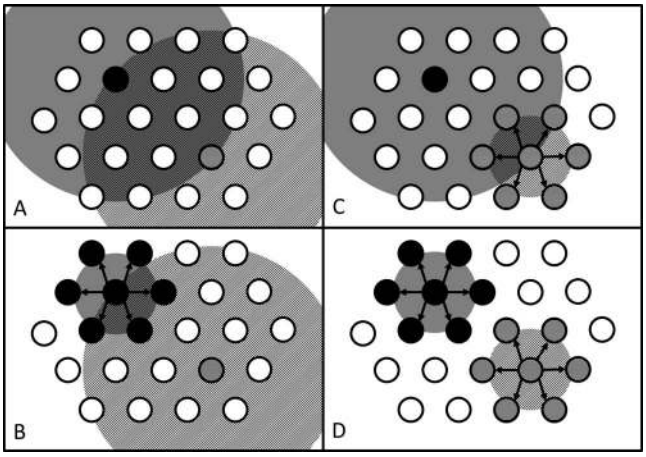

FIGURE 3. Representation of the four interfering paradigms under study. *Solid-filled* electrodes represent active electrodes at the primary stimulation site whereas dashed electrodes represent those activated at the interfering stimulation site. (**A**, **B**) exemplify the expected profile of the electric fields of a monopolar interference (*dashed*) and monopolar and hexapolar stimuli respectively. (**C**, **D**) represent the interference of a hexapolar stimulus (*dashed*) on monopolar and a hexapolar target field respectively.

Alachua, FL, USA) via an 1800 AM-Systems microelectrode amplifier (AM-Systems, Sequim, WA, USA), to record cortical responses from the surface of the brain to 100 repetitions of stimuli, 400 μA in amplitude as described below, from the hexagon closest to and furthest from the area centralis on the suprachoroidal array. Recorded trial-averaged local field potentials were used to identify the approximate location of the cortical representation of the stimulated region of the retina.

The peak activity was mapped to within 1 mm in the exposed area. Then, a 96-channel penetrating recording electrode array (Blackrock Microsystems, Salt Lake City, UT, USA) was pneumatically inserted into the cortex, centered at the region of highest activity in the primary visual cortex identified by the strongest evoked potential with lower latency. The array comprised 10 × 10 channels with 4 corner electrodes disabled, spanning an area of 4 × 4 mm, with each electrode separated by 0.4-mm pitch.

Electrical stimuli were delivered to the stimulating electrode array from a custom stimulator, as described by Jung et al.[25] Additionally, the voltage profile of each stimulation waveform was recorded via a digital multi-meter (DMM) (PXI-4072, National Instruments Corporation, Austin, TX, USA), allowing monitoring of the electrode-tissue interface.

TABLE 1. Combination of Electric Current Ranges of the Stimulation Paradigms at the Primary and Interfering Stimulation Sites

Primary Stimulation Site		Interfering Stimulation Site			
Return	**I (μA)**	**Return**	**I (μA)**	**Return**	**I (μA)**
Monopolar	0–280	Monopolar	0–200	Hexapolar	0–600
Hexapolar	0–630	Hexapolar	0–600	Monopolar	0–200

Stimulation Strategy

Two different suprachoroidal locations, a primary stimulation site (PSS) and an interfering stimulation site (ISS), were stimulated concurrently to evaluate the effects of cross-talk using monopolar and hexapolar configuration returns as illustrated in Figure 3. Two different configurations for adjacent hexagons were possible with the stimulating electrode layout: having a parallel side as shown in Figure 3, or having opposing vertices as in the case in which the hexagons were chosen having the centers over the middle line of the electrode array.

The stimulus profile for the ISS and PSS was standardized as a charge-balanced biphasic, symmetric, constant-current pulse with a phase time of 500 μs and an interphase interval of 10 μs. Interstimulus time was between 800 and 900 ms and current levels were randomized at all times with the same probability. The current levels at the PSS ranged between 0 and 280 μA in steps of 20 μA, and between 0 and 630 μA in steps of 45 μA for monopolar and hexapolar stimulation respectively. On the other hand, current levels at ISS ranged between 0 and 200 μA in steps of 25 μA for monopolar stimulation and between 0 and 600 μA in steps of 75 μA for hexapolar, as described in Table 1. Upper current levels were chosen within the safe injection limit for platinum with sufficient resolution to fit sigmoid curves properly as dictated by experience in a previous report.[9] Each stimulus was repeated 25 times.

Data Analysis

Response signals from all 96 channels of the cortical electrode array were synchronized to the suprachoroidal stimulation delivery using a trigger signal and coordinated via timestamp. Sampling rate was set to 24.4 kHz and data were stored on a personal computer for offline analysis using custom software developed in Matlab 2013b (The MathWorks, Natick, MA, USA). Stimulation artifacts were removed following the algorithm presented by Heffer et al.[26] For each stimulus, 3 ms of the recording (1 ms prestimulus and 2 ms poststimulus) were replaced with linear intermediate voltage values. The data

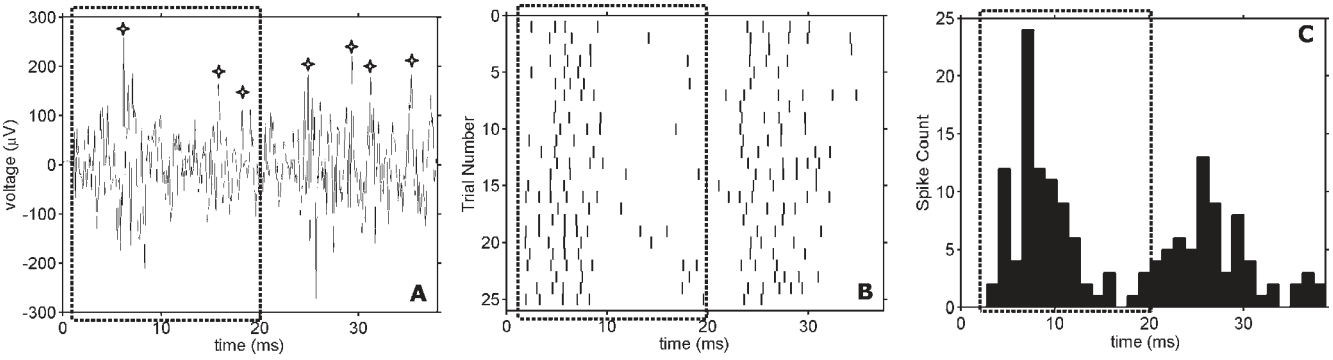

FIGURE 4. (**A**) Shows an example of a typical recording from a cortical electrode channel; stars highlight the occurrence of spikes. (**B**) Illustrates a spike raster ($N = 25$) for the same channel and (**C**) shows a peristimulus histogram. In all cases the stimulus was delivered at $t = 0$. Note that a 20 ms window has been framed in the three panels to illustrate responses under study.

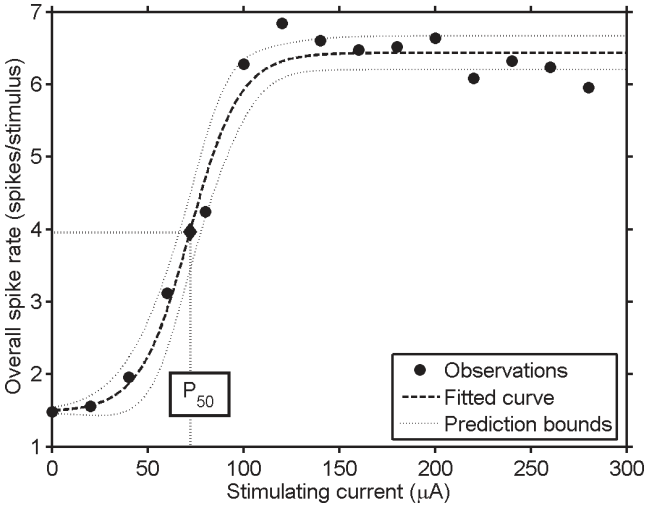

FIGURE 5. Example of sigmoid fit to the cortical activity of the monopolar stimulation delivered at the PSS. The P_{50} value, indicated in the Figure, was 72 μA. Prediction bounds were calculated at the 95% confidence level.

then were band-pass filtered using a zero-phase fifth-order Butterworth filter between 0.3 and 5 kHz.

The root square mean (RMS) of the 100 ms segments of signal preceding each stimulus were calculated for each channel. Recordings were divided into 40-ms epochs starting at the onset of the stimulus delivery for signal processing purposes. Direct activation of RGCs is hypothesized to occur within the first 20 ms, whereas a late response, typically beyond this time interval, is related to activation of photoreceptors and bipolar cells.[27] Spikes were detected using a threshold value set to 3.8 times the overall RMS level of each channel.[8,28] However, the occurrence of each spike within an epoch was binned in intervals of 1 ms and only the first 20 ms after stimulus delivery were considered in this analysis. Figure 4A shows an example of a cortical recording obtained after artifact removal and band-pass filtering. Figures 4B and 4C illustrate a spike raster plot for 25 trials and a peristimulus time histogram respectively obtained from the same recording channel as the response in Figure 4A.

A sigmoidal fit in a least-squares sense of spikes/stimulus relative to the stimulation current was applied to each recording channel of the 96-channel cortical array according to Equation 1:

$$y = Q_0 + \frac{Q_{\max}}{1 + e^{\alpha(P_{50} - x)}} \quad (1)$$

where Q_0 denotes the spontaneous spiking rate (no stimulation), Q_{max} is the maximum spike rate, α is the steepness of the sigmoid, y and x are the spike rate and the stimulating current level, respectively, and P_{50} represents the midpoint of the sloping section of the curve and further defines threshold for purposes of comparison. Figure 5 shows an example of sigmoidal fitting where the activation threshold has been identified. Those channels not exceeding the spontaneous spike rate by at least 1.5 spikes per stimulus at the highest rate under no-interference conditions were considered as non-responding cortical areas and, therefore, removed from the analysis.

The shift of the P_{50} threshold value as a consequence of a concomitant interfering stimulus was defined as a quantitative measure of cross-talk. Thus, linear regression was applied to assess P_{50} shifts at the PSS produced by the interfering stimulation at the ISS.[11] The cross-talk measure was considered as the slope of the regression. Average values were estimated at 95% confidence level. Finally, 1-way ANOVA analysis was performed on the overall threshold shifts to compare cross-talk values. A 95% confidence level was considered as statistically significant.

RESULTS

The overall threshold levels for monopolar and hexapolar stimulation were 44 ± 8 and 61 ± 21 μC·cm^{-2}, respectively. Monopolar P_{50} value was similar to those reported in previous publications and hexapolar P_{50} threshold was overall lower.[9,29] When monopolar interference was applied at the ISS, a drop in the P_{50} value was observed proportional to the stimulus amplitude, as shown in Figure 6. However, interfering hexapolar stimulus did not alter significantly the threshold

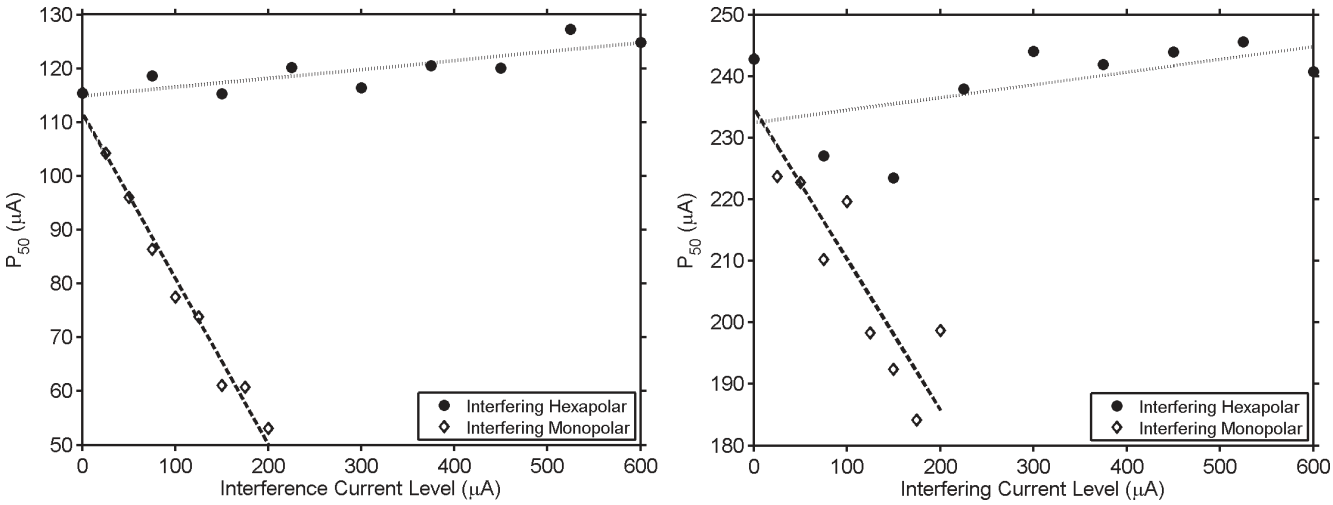

FIGURE 6. Example of the effect of a concomitant monopolar and hexapolar interfering stimulus. *Left* represents the value of the P_{50} threshold when a monopolar stimulus was delivered at the PSS concurrently with a monopolar (*diamond*) and hexapolar (*circle*) interfering stimulus. *Right* shows the P_{50} value when hexapolar stimulation was delivered at the PSS with both, monopolar (*diamond*) and hexapolar (*circle*) interfering on the ISS. Linear regressions for monopolar and hexapolar interference are traced with *dashed* and *dotted lines*, respectively.

Table 2. Overall Correlation Coefficient of Linear Regression Estimated Between Interfering Current Level and P_{50} Value in All Four Scenarios Under Study ($P = 0.95$)

		ISS		
		Monopolar	**Hexapolar**	***N***
PSS	Monopolar	−0.86 ± 0.19	0.25 ± 0.68	4
	Hexapolar	−0.84 ± 0.08	0.21 ± 0.91	3

Table 3. Overall Cross-Talk Value Estimated as the Slope of the Linear Regression of Interfering Current Level and P_{50} Value in All Interference Paradigms ($P = 0.95$)

		ISS		
		Monopolar	**Hexapolar**	***N***
PSS	Monopolar	−0.20 ± 0.08	0.02 ± 0.02	4
	Hexapolar	−0.22 ± 0.03	0.02 ± 0.06	3

level at the PSS. The correlation between the P_{50} value and the current level of the interference was very strong for monopolar stimuli and very weak for hexapolar stimuli, as shown in Table 2.

Cross-talk measures are provided in Table 3 with a 95% confidence level. ANOVA comparisons revealed that the effects of monopolar and hexapolar interference were significantly different ($P < 0.05$). On the other hand, hexapolar interference produced the same threshold shift regardless the type of the stimulus delivered at the PSS ($P = 0.95$). Note that the effect of monopolar interference on the threshold at the PSS did not differ significantly between the cases of monopolar and hexapolar stimulation at the PSS ($P = 0.67$). This suggests that the effect of monopolar interference is similar in both cases, as shown in Figure 7.

The overall cortical effect of concurrent stimulation is illustrated in the heat map of Figure 8, which illustrates the average spike rate recorded in the primary visual cortex in the six scenarios under study; that is, with a monopolar and a hexapolar stimulus at the PSS only, and with the same stimulus plus a concomitant monopolar or hexapolar stimulus delivered at the ISS. Subthreshold monopolar interference increased the spiking rate without altering the morphology of cortical activation, whereas subthreshold hexapolar interference did not alter the cortical activation map.

Discussion

Clinical trials have shown that simultaneous stimulation of the retina has effects on the quality and brightness of the phosphenes elicited by retinal neurostimulation.[30] Shivdasani et al.[10] showed how concurrent multielectrode stimulation, wherein the division of current at different locations was determined by the respective electrode impedances, requires a lower activation threshold in a feline model.[10] However, neural responses produced by stimulation at one site can be distorted by stimuli from different locations as has been found in the case of cochlear implants.[31] In this vein, the present study sheds light on the effects of a concomitant interfering stimulus delivered at a different location by means of independent current sources – in this case using normally sighted cats. Further experiments should consider the use of animals with retinal degeneration or the delivery of intravitreal synaptic blockers.[32]

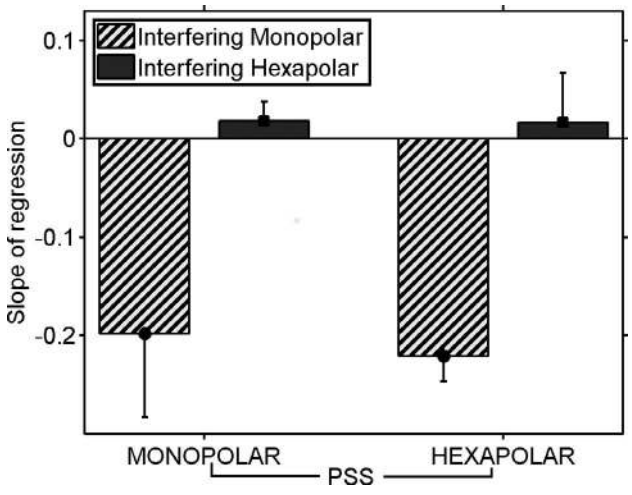

Figure 7. Overall combined estimation of the slope of the linear regression of the P_{50} shift as a function of the interfering current level when monopolar and hexapolar stimuli were delivered at both, the primary site and the interfering site. *Error bars*: Represent the 95% confidence level.

It is clear that hexapolar stimulation provides an efficacious means of isolating concomitant stimulation even for high-current stimuli. In stark contrast to hexapolar interference, significant cross-talk was observed from monopolar interfering currents as small as 25 μA, as illustrated in Figure 6. When an interfering monopolar stimulus was delivered at the ISS, a drop of the P_{50} value of approximately 20% of the interfering level was observed, a finding that is consistent with previously reported results in humans.[30] The effect of the monopolar interference was similar regardless of the return configuration at the PSS. Previous computational models[11] highlighted the pros and cons of interfering stimulation. On the one hand field summation may contribute to decrease activation thresholds.[33] On the other hand excessive cross-talk levels can have a negative effect on visual acuity when delivering parallel stimulation if concomitant stimuli are supra-threshold. Although this study has considered interfering current levels above threshold, reduction of threshold levels will be beneficial if the stimulus remains subthreshold at the ISS. Otherwise, a variation in the cortical activation maps is expected as a consequence of neural interference.[8]

In a previous study, the QMP stimulation paradigm was presented whereby return current was shared between a distant monopolar electrode and a surrounding hexapolar guard.[9] The QMP approach possessed the low-threshold characteristics of monopolar stimulation and the contained and focused retinal activation of hexapolar stimulation. Note that in this study, a similar scenario was presented where concurrent monopolar stimuli were delivered at a different location. The distance between the PSS and ISS electrode locations was effectively between the centers of two adjacent hexagons; that is, 1.63 mm when both hexagons had a parallel side as in Figure 3, and 2.19 mm when hexagons were chosen with facing vertices. Perhaps the most significant finding of this study stems from the observation that monopolar interference produced, in effect, a QMP stimulation even though the monopolar component of the QMP came from a distant and separate source to that of the intended stimulation electrode. Moreover, as mentioned above, the beneficial influence of the interfering electrode could be observed across a distance of at least 2.19 mm. Computational models have suggested a wide spread of the stimulating electric field,[11] which does not have an activation effect on the distant neural targets as in this study – it only contributes to that activation. The axons of distant

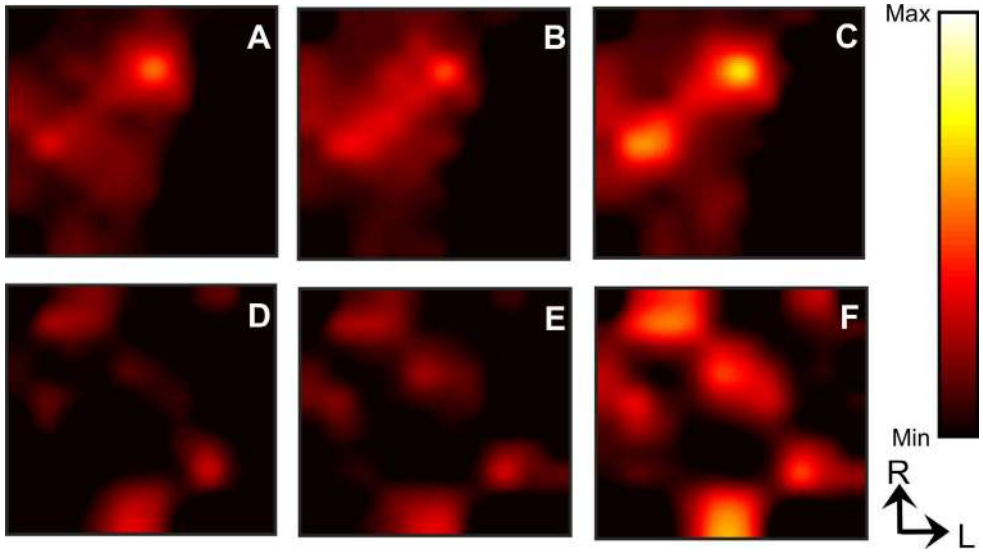

Figure 8. Normalized cortical activation maps obtained in the primary visual cortex using a 96-electrode recording array. Spiking rates were normalized between the spontaneous activity (*black*) and maximum activity (*white*). A 3 × 3 Gaussian filter mask was applied to generate a smoother image. Rostral (R) and lateral (L) directions are indicated in the legend. (**B**, **E**) Illustrate the activation map when a single monopolar and hexapolar stimulus was delivered at the PSS respectively. (**C**, **F**) Show the effect of a concurrent subthreshold monopolar stimulus at the ISS in relation to (**B**, **E**), respectively. (**A**, **D**) Show the effect of a subthreshold hexapolar interference in relation to (**B**, **E**), respectively.

RGCs may extend over an area of stronger field overlapping, hence being exposed to a reinforced cross-talk effect. Please note that owing to proximity to neural targets, this suprachoroidal approach may produce the least pronounced effect of the three retinal approaches, that is, epiretinal, subretinal, and suprachoroidal implants. As this effect would logically produce a broad field that is distributed radially from the interfering electrode, it follows that it would influence many stimulation sites simultaneously. In other words, a significant proportion of the required charge to reach threshold at multiple stimulation sites could be supplied from a single, subthreshold monopolar source reducing the need for individual electrodes to carry the full stimulus charge. This effect could lead to more efficient stimulation, reduced implant power consumption, and the potential to reduce the charge-carrying capacity requirements of individual electrodes, thereby facilitating smaller, more densely packed electrode arrays with diminished risk of reaching electrochemical limitations at the individual electrode-tissue interfaces.

Conclusion

Parallel stimulation appears destined to become an essential component of visual neuroprostheses. To this aim, we have studied the effects of concomitant stimulation through the measurement of cross-talk, a parameter defined as a shift of the activation threshold in response to a distant interfering stimulus. Hexapolar stimulation was highly efficacious in isolating the effects of individual stimulation sites whereas monopolar stimulation produced a reduction of the activation threshold proportional to the strength of the interfering stimulus.

Moreover, it was shown that a concurrent monopolar stimulus can contribute to lower the threshold of several hexapolar stimuli as in the QMP stimulation paradigm wherein the monopolar component has a significant role in cross-talk and the hexapolar component maintains isolation. By introducing a single, broad, subthreshold monopolar field, the thresholds of multiple stimulation sites are reduced simultaneously. This enables the combined focal activation and threshold reduction attributes of QMP stimulation to be realized at multiple sites with only one electrode needing to deliver the monopolar component of QMP. This implementation of multisource stimulation may deliver far-reaching benefit to the field of visual neuroprostheses, and may have use in other areas of neuromodulation.

Acknowledgments

The authors thank Veronika Tatarinoff for assistance during the animal preparation and Barry Gow for assistance with the visual assessment of the fundus.

Supported by the Australian Research Council (ARC) through its Special Research Initiative (SRI) in Bionic Vision Science and the National Health and Medical Research Council (RG1063046).

Disclosure: **P.B. Matteucci**, Medtronics Australasia (E), P; **A. Barriga-Rivera**, None; **C.D. Eiber**, None; **N.H. Lovell**, None; **J.W. Morley**, None; **G.J. Suaning**, P

References

1. Suaning G, Lovell N, Lehmann T. Neuromodulation of the retina from the suprachoroidal space: The Phoenix 99 implant. In: *IEEE 2014 Biomedical Circuits and Systems Conference (BioCAS) - Proceedings*. Piscataway, NJ: IEEE; 2014:256–259.
2. Ayton LN, Blamey PJ, Guymer RH, et al. First-in-human trial of a novel suprachoroidal retinal prosthesis. *PLoS One*. 2014;9:e115239.
3. Weiland J. Visual prosthesis, epiretinal devices. *Encyclop Comput Neurosci*. 2015;3123–3125.
4. Shivdasani MN, Sinclair NC, Dimitrov PN, et al. Factors affecting perceptual thresholds in a suprachoroidal retinal prosthesis. *Invest Ophthalmol Vis Sci*. 2014;55:6467–6481.
5. Humayun MS, Dorn JD, da Cruz L, et al. Interim results from the international trial of Second Sight's visual prosthesis. *Ophthalmology*. 2012;119:779–788.
6. Eiber CD, Lovell NH, Suaning GJ. Attaining higher resolution visual prosthetics: a review of the factors and limitations. *J Neural Eng*. 2013;10:011002.

7. Stronks HC, Dagnelie G. The functional performance of the Argus II retinal prosthesis. *Expert Rev Med Devic*. 2014;11:23–30.
8. Dumm G, Fallon JB, Williams CE, Shivdasani MN. Virtual electrodes by current steering in retinal prostheses. *Invest Ophthalmol Vis Sci*. 2014;55:8077–8085.
9. Matteucci PB, Chen SC, Tsai D, et al. Current steering in retinal stimulation via a quasimonopolar stimulation paradigm. *Invest Ophthalmol Vis Sci*. 2013;54:4307–4320.
10. Shivdasani MN, Fallon JB, Luu CD, et al. Visual cortex responses to single-and simultaneous multiple-electrode stimulation of the retina: implications for retinal prostheses. *Invest Ophthalmol Vis Sci*. 2012;53:6291–6300.
11. Moghadam GK, Wilke R, Suaning GJ, Lovell NH, Dokos S. Quasi-monopolar stimulation: a novel electrode design configuration for performance optimization of a retinal neuroprosthesis. *PLoS One*. 2013;8:e73130.
12. Abramian M, Lovell NH, Habib A, Morley JW, Suaning GJ, Dokos S. Quasi-monopolar electrical stimulation of the retina: a computational modelling study. *J Neural Eng*. 2014;11:025002.
13. Habib AG, Cameron MA, Suaning GJ, Lovell NH, Morley JW. Spatially restricted electrical activation of retinal ganglion cells in the rabbit retina by hexapolar electrode return configuration. *J Neural Eng*. 2013;10:036013.
14. Firszt JB, Koch DB, Downing M, Litvak L. Current steering creates additional pitch percepts in adult cochlear implant recipients. *Otol Neurotol*. 2007;28:629–636.
15. Koch DB, Downing M, Osberger MJ, Litvak L. Using current steering to increase spectral resolution in CII and HiRes 90K users. *Ear Hearing*. 2007;28:38S–41S.
16. Litvak LM, Spahr AJ, Emadi G. Loudness growth observed under partially tripolar stimulation: model and data from cochlear implant listeners. *J Acoust Soc Am*. 2007;122:967–981.
17. Wilke R, Moghadam GK, Lovell N, Suaning G, Dokos S. Electric crosstalk impairs spatial resolution of multi-electrode arrays in retinal implants. *J Neural Eng*. 2011;8:046016.
18. Wong Y, Chen S, Seo J, Morley J, Lovell N, Suaning G. Focal activation of the feline retina via a suprachoroidal electrode array. *Vision Res*. 2009;49:825–833.
19. Landsberger DM, Padilla M, Srinivasan AG. Reducing current spread using current focusing in cochlear implant users. *Hearing Res*. 2012;284:16–24.
20. Schmid EW, Fink W, Wilke R. Simultaneous vs. sequential and unipolar vs. multipolar stimulation in retinal prostheses. *IEEE/EMBS 6th International Conference on Neural Engineering (NER)*. Piscataway, NJ: IEEE; 2013:190–193.
21. Suaning G, Hallum L, Preston P, Lovell N. An efficient multiplexing method for addressing large numbers of electrodes in a visual neuroprosthesis. *26th Annual International Conference of the IEEE Engineering in Medicine and Biology Society*. Piscataway, NJ: IEEE; 2004:4174–4177.
22. Dodds C, Schuettler M, Guenther T, Lovell N, Suaning G. Advancements in electrode design and laser techniques for fabricating micro-electrode arrays as part of a retinal prosthesis. *33rd Annual International Conference of the IEEE Engineering in Medicine and Biology Society*. Piscataway, NJ: IEEE; 2011:636–639.
23. Schuettler M, Stiess S, King B, Suaning G. Fabrication of implantable microelectrode arrays by laser cutting of silicone rubber and platinum foil. *J Neural Eng*. 2005;2:S121.
24. Tusa R, Palmer L, Rosenquist A. The retinotopic organization of area 17 (striate cortex) in the cat. *J of Comp Neurol*. 1978;177:213–235.
25. Jung LH, Shany N, Emperle A, et al. Design of safe two-wire interface-driven chip-scale neurostimulator for visual prosthesis. *IEEE J Solid-St Circ*. 2013;48:2217–2229.
26. Heffer LF, Fallon JB. A novel stimulus artifact removal technique for high-rate electrical stimulation. *J Neurosci Meth*. 2008;170:277–284.
27. Elfar SD, Cottaris NP, Raymond A, Gary W. A cortical (V1) neurophysiological recording model for assessing the efficacy of retinal visual prostheses. *J Neurosci Methods*. 2009;180:195–207.
28. Cicione R, Fallon JB, Rathbone GD, Williams CE, Shivdasani MN. Spatiotemporal interactions in the visual cortex following paired electrical stimulation of the retina visual cortex response to paired stimulation of retina. *Invest Ophthalmol Vis Sci*. 2014;55:7726–7738.
29. Cicione R, Shivdasani MN, Fallon JB, et al. Visual cortex responses to suprachoroidal electrical stimulation of the retina: effects of electrode return configuration. *J Neural Eng*. 2012;9:036009.
30. Horsager A, Greenberg RJ, Fine I. Spatiotemporal interactions in retinal prosthesis subjects. *Invest Ophthalmol Vis Sci*. 2010;51:1223.
31. Loizou PC. Mimicking the human ear. *IEEE Signal Proc Mag*. 1998;15:101–130.
32. Schallek J, Kardon R, Kwon Y, Abramoff M, Soliz P, Ts'o D. Stimulus-evoked intrinsic optical signals in the retina: pharmacologic dissection reveals outer retinal origins. *Invest Ophthalmol Vis Sci*. 2009;50:4873–4880.
33. McCreery DB, Agnew WF, Bullara LA. The effects of prolonged intracortical microstimulation on the excitability of pyramidal tract neurons in the cat. *Ann Biomed Eng*. 2002;30:107–119.

Investigative Ophthalmology & Visual Science